ORIGINAL ARTICLE

Application of Gleason analogous grading system and flow cytometry DNA analysis in a novel knock-in mouse prostate cancer model

G Wu, Lei Yu, L Wang, H Wang, J W Xuan

Postgrad Med J 2006;**82**:40–45. doi: 10.1136/pgmj.2005.038042

See end of article for authors' affiliations

Correspondence to: Dr G Wu and Dr H Wang, Department of Urology, Xijing Hospital, the Fourth Military Medical University, Xi'an, China, 710032; wuguojun@fmmu.edu.cn; dusxjhw@fmmu.edu.cn

Submitted 5 June 2005
Accepted 17 July 2005

Objective: A new knock-in mouse adenocarcinoma prostate model (KIMAP) was established, which showed a close to human kinetics of tumour development. This study used a new mouse histological grading system similar to the human Gleason grading system and flow cytometry DNA analysis to measure and compare the new KIMAP model with human CaP and transgenic mouse adenocarcinoma prostate (TGMAP) model.

Methods: According to heterogeneity of the clinical standard for prostate cancer diagnosis, a close to human mouse standard for histological grading and scoring system, Gleason analogous grading system, was established in this study. Sixty KIMAP and 48 TGMAP prostate cancer samples were measured and compared with human CaP. Flow cytometry DNA analysis was performed on malignant prostate tissues obtained from both TGMAP and KIMAP models.

Results: Mice with CaP from KIMAP (n = 60) and TGMAP (n = 48) models showed a different distribution of histological scores (p = 0.000). KIMAP mice showed higher percentage (53.3%) of compound histological score rate than TGMAP (25%), but closer to the human clinical average (50%), which showed significant correlation with age (p = 0.001), while TGMAP mice showed unbalanced and random score distribution in all age groups. Flow cytometry analyses showed that most tumour tissues in KIMAP were diploid, analogous to the human condition, while all the TGMAP mice showed aneuploid tumours.

Conclusions: Results of this study further show that KIMAP, a new generation of murine prostate cancer model, could be used as a supplementary model in addition to the currently widely used transgenic models.

Mice and other rodents do not spontaneously develop prostate cancer. For this reason, the development of genetically engineered mouse prostate cancer (CaP) models is critical for pre-clinical studies of CaP, the most common cancer in men in North America.[1–10] Prostate secretory protein of 94 amino acids (PSP94), also known as β-microseminoprotein, like human prostate specific antigen (PSA), is one of the most abundantly expressed secretory proteins in human prostatic fluid and semen.[11 12] Raised serum concentrations of PSA and PSP94 proteins were identified and used as serum markers for the diagnosis and prognosis of CaP. In contrast with PSA, which has no equivalent in rodent species, PSP94 analogues from studies in humans, primates, pigs, and rodents have showed that PSP94 is a conserved, but also a rapidly evolving protein.[13–16]

We have previously established the transgenic mouse adenocarcinoma of the prostate (TGMAP) model directed by a PSP94-gene promoter/enhancer region and a new knock-in mouse adenocarcinoma of the prostate (KIMAP) model line at the PSP94 gene locus.[17 18] The new KIMAP model had several advantages over the traditional transgenic models, such as prolonged tumour growth, a predominance of well and moderately differentiated tumours, highly synchronous prostate cancer development, and highly stable phenotype and genotype.[18] In this study, we used a new mouse histological grading system (Gleason analogous grading system) similar to the human Gleason grading system and flow cytometry DNA analysis to measure and compare the new KIMAP model with human CaP and the PSP94 gene directed TGMAP model.

METHODS

Mouse anatomy and identification

All animal experiments were conducted according to standard protocols. Transgenic (PSP-TGMAP) mice were identified by a quick PCR genotyping protocol as previously reported.[17] Breeding of transgenic mice was all carried out in strains of F1 hybrids (C57BL/6 x CBA), first by mating with the wild type then gradually by mating among transgenic mice. All KIMAP mice breeding lines were mostly established in the CD1 or 129Sv background, and C57 BL6 back ground was also tested with no strain differences. Genotyping was performed by a fast PCR genotyping as previously reported.[18] Primer pairs used for screening for germline progenies from chimeras by PCR genotyping were as previously reported.[17 18]

The prostate along with the male accessory glands—that is, the ventral and dorsolateral prostate lobes (VP, DLP respectively), seminal vesicles (SV) and coagulation gland (CG, or AP, the anterior gland)—were dissected out separately as per the description and definition reported.[15 17]

Definitions of various grades of CaP

To study tumour development in the genetically engineered PSP knock-in (KIMAP) and transgenic (PSP-TGMAP) models, some modifications were adopted according to the established diagnostic criteria previously reported.[19–21]

Abbreviations: KIMAP, knock-in mouse adenocarcinoma prostate; TGMAP, transgenic mouse adenocarcinoma prostate; PSA, prostrate specific antigen

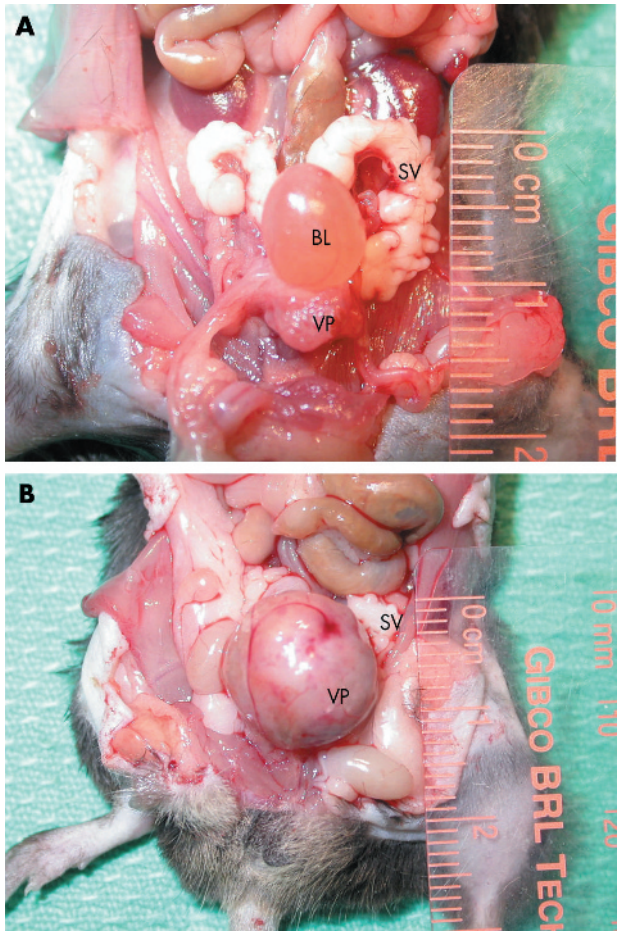

Figure 1 Anatomy and gross pathology of KIMAP and TGMAP mice. (A) Maccroscopic examination of a KIMAP mouse 52 weeks of age after prolonged CaP development showing a 0.3 g VP tumour. (B) Macroscopic examination of a TGMAP mouse 20 weeks of age showing a 5 g VP tumour. KIMAP, knock-in mouse adenocarcinoma prostate; TGMAP, transgenic mouse adenocarcinoma prostate; VP, ventral prostate; DLP, dorsolateral prostate, BL, bladder; SV, seminal vesicles.

According to heterogeneity of the clinical standard for prostate cancer diagnosis, a close to human mouse standard for histological grading and scoring system were established in this study. We termed this system the Gleason analogous grading system. The architectural patterns of adenocarcinoma seen were assessed by five different histological grades: grade 1 (very well differentiated): single, separate, uniform glands closely packed, with definite boundaries; grade 2 (well differentiated): single, separate uniform glands loosely packed, with irregular edges; grade 3 (glands with variable and distorted architecture): single, separate, uniform scattered glands and smoothly circumscribed papillary/cribriform masses; grade 4 (poorly differentiated): cribriform masses with ragged, invading edges and fused glands; grade 5 : non-glandular solid, rounded masses of cells; cribriform architecture with foci of central necrosis (known as comedocarcinoma) and undifferentiated anaplastic carcinomas. Based on the most prevalent histological grade (''the primary pattern/grade'') and the second most prevalent histological pattern (''secondary pattern/grade''), the new mouse scoring system was derived by adding the primary pattern grade number to the secondary grade number. If only one pattern is seen throughout, the score is derived by the doubling ''grade'' number.

Flow cytometry

Flow cytometry DNA analysis was performed on malignant prostate tissues obtained from both TGMAP (n = 8) and KIMAP models (n = 9), which were either freshly excised or snap frozen in liquid nitrogen. Single cell suspensions were prepared according to the standard clinical procedures in our hospital. Before analysis, each cell suspension was filtered through a nylon mesh to remove any debris and cell aggregates. Normal mouse spleen lymphocytes were dissociated and used as a control to establish the normal diploid DNA peak position. All samples were analysed with EPICS C flow cytometer (Coulter Electronics, Hialeah, FL). The resultant single nuclei suspension was treated with ribonuclease and stained with 50 g/ml propidium iodide (Beckman Coulter, Miami, FL). DNA histograms were classified as diploid, tetraploid, or aneuploid. DNA aneuploidy was defined by the presence of a tumour population with a definable G0/G1 peak that was distinct from the diploid population. Tetraploidy was defined by a peak with a DNA index (ratio of the channel number of the abnormal to the diploid population) of between 1.9 and 2.1. DNA proliferation was measured by flow cytometry as values of % S (per cent S-phase) and % S +% G_2M (per cent S-phase and G_2M phase) separately.[22]

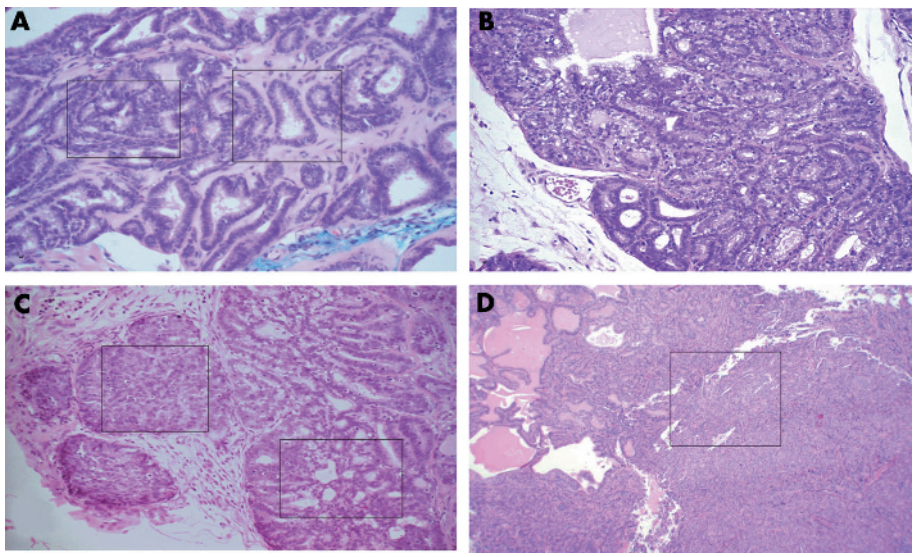

Figure 2 Histological analysis of KIMAP prostate cancer models by a new mouse Gleason analogous grading system established in this study. Sections were stained with haematoxylin and eosin (H and E). (A) Histological score 5 from a KIMAP mouse at age 30 weeks. Two boxes showed histological grade 2 (right) and 3 (left) tumour foci. H and E ×25. (B) Histological score 6 (histological grades 3 + 3) from a KIMAP mouse at age 30 weeks. H and E ×25. (C) Histological score 7 (3 + 4) from a KIMAP mouse at age 45 weeks. Right area: grade 3, small acinar infiltrating the stroma. Left area: grade 4 showing cribriform acini. H and E ×10. (D) Histological score 9 (4 + 5) from KIMAP at age 67 weeks. Boxed area: grade 5. Left area: grade 4. H and E ×10.

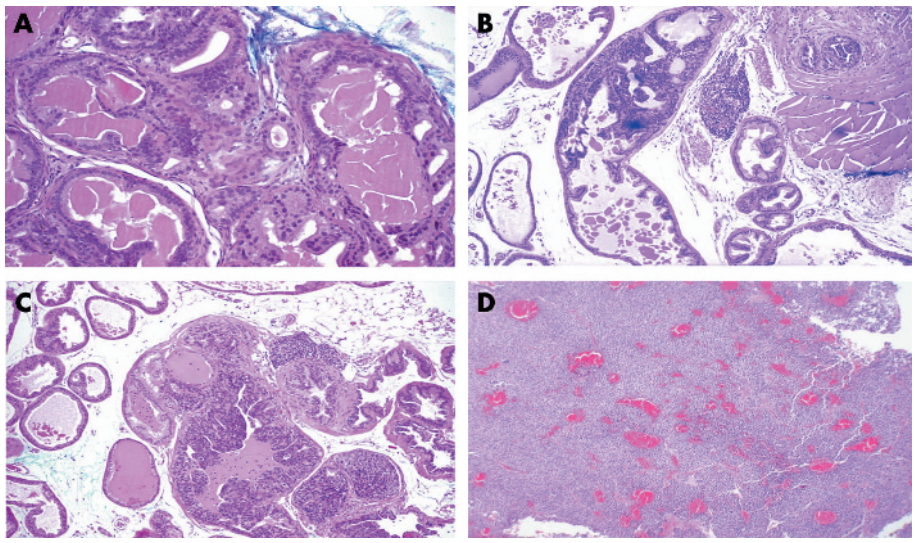

Figure 3 Histological analysis of TGMAP prostate cancer models by a new mouse Gleason analogous grading system established in this study. Sections were stained with haematoxylin and eosin (H and E). (A) Histological score 6, from a TGMAP mouse at age 34 weeks (histological grade 3). H and E ×10. (B) Histological score 8, from a TGMAP mouse at age 26 weeks showing heterogeneity (3 + 5 grades) with low extent tumour foci of undifferentiated anaplastic mass (5) and papillary malignant acini (3). H and E ×10. (C) H istological score 9 from TGMAP at age 30 weeks showing heterogeneity (histological grades 4 + 5) with low extent tumour foci of solid masses (5) and cribriform malignant acini (4). H and E ×10. (D) Histological score 10 (5 + 5) from TGMAP mice at age 32 weeks showing high extent of tumour foci of undifferentiated anaplasia (GE histological grade 5). H and E ×10.

Statistical analysis

SPSS 10 and Sigma Plot 2000 softwares were used for all analysis, including χ^2, Mann-Whitney tests, etc.

RESULTS

Distribution of the mouse histological grades and scores

A comparative study with mice from both KIMAP and TGMAP prostate cancer models (shown in fig 1) was performed. To differentiate heterogeneity of the architecture of GE mouse prostate tumour, we established a new mouse histological grading system similar to the human Gleason grading system. Each mouse with CaP in both models of KIMAP (n = 60) and TGMAP (n = 48) was assigned with the mouse Gleason analogous grading system (fig 2A, B, C, D, shown by boxes), a combination of a primary GE histological grades (a dominant grade) and a secondary grade (the non-dominant grade). In general, because of the poor heterogeneity, TGMAP mice were not applicable to this clinical oriented system. The classification of CaPs in TGMAP mice was followed only by similarities (fig 3A, B, C, D). The distribution of the mouse histological scores in KIMAP and TGMAP was plotted in fig 4A. In KIMAP mice, mouse histological scores were more evenly distributed than TGMAP in all 4–9 ranges except the score 10 (doubling grades 5+5, fig 3D). Most scores in KIMAP were score 9 (28.3%) and 6 (23.3%), other scores were 4 (5.0%), 5 (5.0%), 7 (20.0%) and 8 (18.3%). In contrast, mouse histological scores in TGMAP were all distributed in higher score ranges (6–10), with no medium range of mouse histological scores 4 and 5 (see fig 2A). Most scores in TGMAP were at the highest sores 10 (60.4%, fig 3D). The difference in mouse histological score distribution between KIMAP and TGMAP models is highly significant (p = 0.000).

Compound mouse histological score rates

The significant differences of the tumour architectural heterogeneity between the TGMAP and KIMAP models were further characterised by the percentage of the compound histological score rate, which was designated as the proportion (%) of mice with the compound histological scores (combination of two unequal histological grades) in total CaP mice (shown in boxes of fig 2 and fig 3). The main reason to introduce this parameter in this study is that most (36 of 48) of TGMAP mice showed no compound histological scores, because of poor heterogeneity (fig 3). The average% compound histological score rate in KIMAP is 53.3% (n = 60), which is close to the reported clinical average (50%, table 1) and is higher than TGMAP mice (25%, n = 48, table 1).[20 21] Figures 2 and 3 show the assessment of compound mouse histological score 5 (2+3, fig 2A), 7 (3+4, fig 2C), and 9 (4+5, fig 2D) in KIMAP mice; 8 (3+5, fig 3B) and 9 (4+5, fig 3C) in TGMAP mice.

Next, we determined the correlation of % compound score rate with the age, meanwhile we also determined the starting age for this process resulting in the different % compound histological score rate in these two models. The distribution of the% compound histological score rate (fig 4B) was plotted against different age groups. In TGMAP mice, only 12 of 48 mice showed compound histological scores, and were found distributed in age groups (19–26, 27–34, and 35–43 weeks) at rates of 4 of 12, 7 of 25, and 1 of 5 respectively (fig 4B). In contrast with TGMAP, most KIMAP mice (32 of 60) showed higher% compound scores, distributed in age groups (from 12 weeks of age) at rates of 25% (12–18 weeks), 31.3% (19–26 weeks), 37.5% (27–34 weeks), 55.6% (35–43 weeks), and 78.3% (>43 weeks) respectively (fig 4B). KIMAP mice showed a trend of increase of the compound score rate and correlated with age (p = 0.001, fig 4B).

Flow cytometry studies

To further differentiate the two murine models at the chromosomal level, flow cytometry experiments were performed. Visible, homogenous prostate tumours were collected from only late stage mice. Diploid control tissue samples were obtained from mouse normal spleen tissue cells (fig 5A). All of eight TGMAP tumours showed aneuploid changes (fig 5B and C, table 1). Figure 5B shows tumour samples mixed with internal control samples and figure 5C is the neat test without a control sample. The first peak, C, is the diploid. Peak D is the aneuploid. In the nine KIMAP tumour samples analysed, eight mice showed mostly diploid tumour peaks (89%, fig 5D and E) and only one mouse had a tetraploid peak (11%, fig 5F), which approximates the results of flow cytometry in clinical CaP investigation (75% diploid and 25% non-diploid tumour,[22] table 1). Figure 5D and E showed results of the mixture (sample + spleen) and neat (without spleen control) tests separately.

Through flow cytometry tests, the DNA proliferation rate (% S and% S +% G_2M) of KIMAP and TGMAP mice was

Table 1 Pathology features of KIMAP mice comparing TGMAP mice and human clinical data

	PSP-KIMAP	PSP-TGMAP	Human[20–22]
Architecture of tumour foci			
Heterogeneity	High	Low	High
Histological score (%)			
⩽4	5.0	0	14.3
5	5.0	0	15.3
6	23.3	10.4	42.2
7	20.0	22.9	19.1
⩾8	46.7	66.7	9.2
Mean score	7.3	8.8	5.6
% Compound histological scores	53.3	25	50
DNA ploidy by flow cytometry			
Diploidy (%)	88.9	0	75.0
Anuploidy(%)	0	100.0	4.0
Tetrodiploidy (%)	11.1	0	21.0
%S by flow cytometry	3.6	17.3	3.1
%S +%G_2M by flow cytometry	10.7	23.0	10.5

KIMAP, knock-in mouse adenocarcinoma prostate; TGMAP, transgenic mouse adenocarcinoma prostate; %S, per cent of the cells of S-phase; %S +%G_2M, per cent of the cells of S phase and G_2M phase.

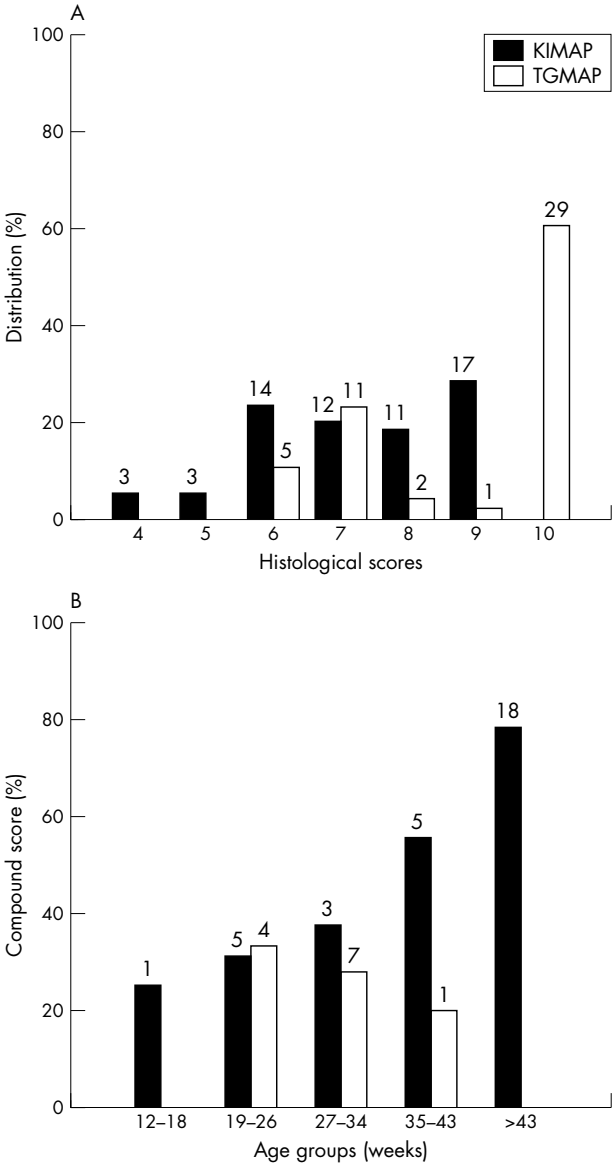

assessed. The average % S and% S +% G_2M of TGMAP mice were 17.3% and 23.0%, while KIMAP mice had % S and % S + % G_2M values of 3.6% and 10.7% respectively, which more closely reflects the DNA proliferation rate in clinical report (being 3.1% and 10.5% respectively,[22] table 1).

DISCUSSION

Because of the biological heterogeneity of CaP, further understanding of the biology of CaP is necessary before significant advances in treatment can be developed. Insight into the epigenetic events and cellular interactions between CaP cells and the organ microenvironment will be critical. Continued empirical treatment is unlikely to provide the therapeutic advances required to improve outcomes for patients with CaP. The use of animal models may provide an in vivo system to permit the study of CaP biology. CaP continues to be the second leading cause of cancer related death among men. To develop more fully effective prevention and intervention strategies for this prevalent disease, the underlying molecular mechanisms of initiation, progression, and metastatic spread must be understood. To this end mouse models have an essential role in CaP research in that they can closely mimic the pathological and biochemical features of the disease.

A mouse model mimicking human CaP must show the following features that are characteristic of human CaP: correlation with increasing age; high incidence rate; slow growth rate; a histological CaP structure of a majority of well to moderately differentiation; androgen dependence, and initial responsiveness to hormone therapy followed by the development of refractoriness to androgen ablation therapy, and high propensity for bone metastasis.

The knock-in mouse prostate cancer model is a mouse model resulting from a single endogenous knock-in mutation under the control of the promoter/enhancer region of the

Figure 4 Comparison of histological scores (compound score percentage) between TGMAP and KIMAP mice. (A) Comparison of the distribution of histological scores between KIMAP and TGMAP models. Numbers listed above each bar on the graph show the number of mice with the identified histological scores. Percentage (y axis) shows the % of mice with the identified histological scores of the total mice tested. (B) Plot of the compound histological scores percentages (% of histological scores composed of different primary and secondary scores) against age groups. Numbers listed above each bar show the number of mice of that age group with the identified compound score rate (%).

prostate specific gene PSP94. One of the unique features of this PSP-KIMAP model is the presence of sufficient heterogeneity to allow for the application of a system similar to that of the human Gleason histological grading system, the system widely used clinically for the grading of human prostate cancer.[20 21] We have termed this system, created for purposes of our study, the Gleason analogous grading system. The most prevalent range of Gleason analogous grades (3–4) and Gleason analogous scores (5–7/10) were the same in PSP-KIMAP mice as in human CaP cases.[21] Additionally, a significant correlation of Gleason analogous grades and scores with animal age was seen. KIMAP mice also had a higher percentage of compound histological scores, which is more analogous to human CaP. Flow cytometry study of DNA ploidy and proliferation showed that most KIMAP mouse tumour cells were diploid, as in human CaP.[22] In contrast, most of TGMAP mice were aneuploid.

The Gleason grading system is based on the degrees of architectural differentiation and has been advocated as a way to improve the pathologists' ability to accurately diagnose and prognosticate the biological behaviour of a particular tumour. This system effectively detects the full range of human CaP development. Other systems in use internationally are the Mostofi (World Health Organisation) and Boking systems. These grading systems can identify well differentiated and poorly differentiated adenocarcinomas, but are less successful in the subdividing of moderately differentiated adenocarcinomas.

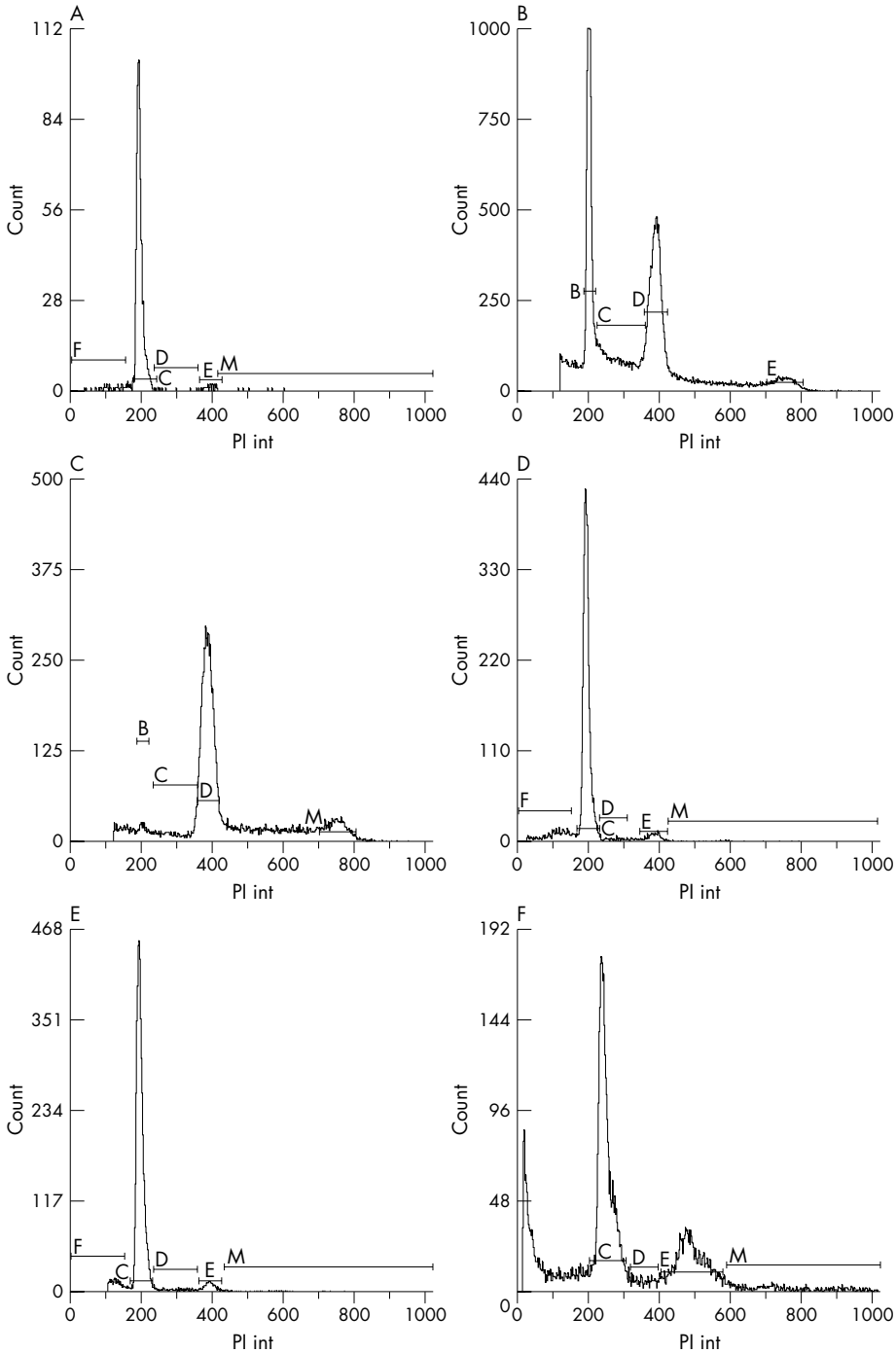

Figure 5 Flow cytometry analyses of late stage CaP samples from both KIMAP and TGMAP models. All diagrams are singlet pictures, with cell counts (y xis) plotted against PI int (propidium iodide). (A) Normal spleen tissue dissociated cells from KIMAP mice (control for diploid). (B) Mixture of spleen and CaP cells of TGMAP mice showing aneuploidy (spleen cells serve as internal control for diploid). (C) Neat test of CaP cells of TGMAP mice showing aneuploidy. (D) Mixture of spleen and tumour cells of KIMAP mice showing diploid. (E) Neat test of CaP cells of KIMAP mice showing diploid. (F) Neat test of CaP cells of KIMAP mice showing tetraploid changes (peak E). Peaks were shown as C (cell cycle phase G_0/G_1, for diploid), D (S phase for aneuploidy), E (G_2M phase for tetraploid) separately.

Any mouse CaP models cannot be applied to pre-clinical studies if they do not show all of the histopathological patterns of CaP. None of the previous transgenic CaP models have shown features that would qualify them for classification by the Gleason analogous grading system. However, all previous transgenic models can only be characterised by a ''crude,'' non-clinically relevant histological grading system,[23] partly because of the lack of sufficient heterogeneity, rare patterns of neoplastic change. The PSP- TGMAP mice showed predominantly tumours with high grades (5) and very high scores (8–10/10), without a full range of Gleason grading and score distribution.

A steady, prolonged tumour growth (most being moderately differentiated adenocarcinoma) starting after puberty is the prerequisite for the establishment of such an experimental mouse CaP model that is applicable to the Gleason analogous grading system, features that are present in PSP-KIMAP mice. As compared with the transgenic model, the fast, uncontrolled, and exponential tumour growth in late stage puberty is the most common pattern for PSP-TGMAP. In most cases, the tumour grows rapidly to a large size in a short time frame (sometimes in as little as two weeks) up to about 15 g, while the total body mass is only 35 g. This is a typical artefact of a forced manipulation of the promoter driving tumour inducer gene in the CaP model. Furthermore, this fast, ''uncontrolled'' CaP growth decreases the relevance of the Gleason analogous grading system.

One of the reasons that accounts for the fact that all previous transgenic models are incongruous with clinical standards for the identification of experimental mouse cancers are the limitations of the transgenic technique itself. When compared with the rodent Nobel and reconstituted prostate CaP models, the transgenic CaP model shows the inheritability and reproducibility of many salient features of CaP in all progenies. However, it is still an empirical model.

The PSP-KIMAP showed a fundamental similarity to the human situation in its histopathological characteristics. The simplest theoretical explanation for this is that none of the previously described transgenic CaP models is fully regulatable because of an endogenous knock-in mutation by a prostate specific gene. The knocked insertion of the PSP94 gene confers upon the PSP-KIMAP model a high regularity, as it only knocks in a SV40 Tag in the PSP94 structural gene and no regulatory factors/regions will be affected. The PSP94 gene promoter is a strong, prostate tissue specific promoter, and the SV40 Tag is coupled with the full capacity of a promoter of the most abundant prostate secretory gene.

As with all genetically engineered prostate cancer models, the adoption of mouse specific histopathological standard could not be directly applied to human clinical diagnosis or prognosis. However, the PSP-KIMAP model that most closely mimics human CaP may show great similarities of tumour development and may lay down the foundation for the use of PSP-KIMAP mouse models, eventuating in novel human CaP therapeutic approaches.

ACKNOWLEDGEMENTS

We thank all the staff in the Surgery Lab of University of Western Ontario for their participation in this study: Manal Y Gabril, Conghui Guo MD PhD, Wenming Duan MD PhD.

Authors' affiliations
G Wu, L Yu, L Wang, H Wang, Department of Urology, Xijing Hospital, the Fourth Military Medical University, Xi'an, China
G Wu, J W Xuan, Department of Surgery, University of Western Ontario, London, Ontario, Canada

Conflict of interests: G J Wu has been paid by the Fourth Military Medical University for running educational programmes and financial support for attendance at scientific meetings.

The first three authors contributed equally to this work.

REFERENCES

1 **Abate-Shen C**, Shen MM. Mouse models of prostate carcinogenesis. *Trends Genet* 2002;**18**:S1–5.
2 **Huss WJ**, Maddison LA, Greenberg NM. Autochthonous mouse models for prostate cancer: past, present and future. *Semin.Cancer Biol* 2001;**11**:245–60.
3 **Winter SF**, Cooper AB, Greenberg NM. Models of metastatic prostate cancer: a transgenic perspective. *Prostate Cancer Prostatic Dis* 2003;**6**:204–11.
4 **Green JE**, Greenberg NM, Ashendel CL, *et al.* Workgroup 3: transgenic and reconstitution models of prostate cancer. *Prostate* 1998;**36**:59–63.
5 **Killion JJ**, Radinsky R, Fidler IJ. Orthotopic models are necessary to predict therapy of transplantable tumours in mice. *Cancer Metastasis Rev* 1998;**17**:279–84.
6 **Masumori N**, Thomas TZ, Chaurand P, *et al.* A probasin–large T antigen transgenic mouse line develops prostate adenocarcinoma and neuroendocrine carcinoma with metastatic potential. *Cancer Res* 2001;**61**:2239–49.
7 **Maroulakou IG**, Anver M. Garrett L, *et al.* Prostate and mammary adenocarcinoma in transgenic mice carrying a rat C3(1) simian virus 40 large tumour antigen fusion gene. *Proc Natl Acad Sci U S A* 1994;**91**:11236–40.
8 **Garabedian EM**, Humphrey PA, Gordon JI. A transgenic mouse model of metastatic prostate cancer originating from neuroendocrine cells. *Proc Natl Acad Sci U S A* 1998;**62**:227–37.
9 **Perez-Stable C**, Altman NH, Mehta PP, *et al.* Prostate cancer progression, metastasis, and gene expression in transgenic mice. *Cancer Res* 1997;**57**:900–6.
10 **Ellwood-Yen K**, Graeber TG, Wongvipat J, *et al.* Myc-driven murine prostate cancer shares molecular features with human prostate tumours. *Cancer Cell* 2003;**4**:223–38.
11 **Hara M**, Kimura H. Two prostate-specific antigens, g-seminoprotein and h-microseminoprotein. *J Lab Clin Med* 1989;**113**:541–8.
12 **Abrahamsson PA**, Lilja H, Falkmer S, *et al.* Immunohistochemical distribution of the three predominant secretory proteins in the parenchyma of hyperplastic and neoplastic prostate glands. *Prostate* 1988;**12**:39–46.
13 **Hyakutake H**, Sakai H, Yogi Y, *et al.* Beta-microseminoprotein immunoreactivity as a new prognostic indicator of prostatic carcinoma. *Prostate* 1993;**22**:347–55.
14 **Xuan JW**, Kwong J, Chan FL, *et al.* cDNA, genomic cloning and gene expression analysis of mouse PSP94 (prostate secretory protein of 94 amino acids). *DNA Cell Biol* 1999;**18**:11–26.
15 **Imasato Y**, Onita T, Moussa M, *et al.* Rodent PSP94 gene expression is more specific to the dorsolateral prostate and less sensitive to androgen ablation than probasin. *Endocrinology* 2001;**142**:2138–46.
16 **Lazure C**, Villemure M, Gauthier D, *et al.* Characterization of ostrich (Struthio camelus) beta-microseminoprotein (MSP): identification of homologous sequences in EST databases and analysis of their evolution during speciation. *Protein Sci* 2001;**10**:2207–18.
17 **Gabril MY**, Onita T, Ji PG, *et al.* Prostate targeting:PSP94 gene promoter/enhancer region directed prostate tissue-specific expression in a transgenic mouse prostate cancer model. *Gene Therapy* 2002;**9**:1589–99.
18 **Duan W**, Gabril MY, Moussa M, *et al.* Knockin of SV40 Tag oncogene in a mouse adenocarcinoma of the prostate model demonstrates advantageous features over the transgenic model. *Oncogene* 2005;**24**:1510–24.
19 **Shappell SB**, Thomas GV, Roberts RL, *et al.* Prostate pathology of genetically engineered mice: definitions and classification. The consensus report from the Bar Harbor meeting of the Mouse Models of Human Cancer Consortium Prostate Pathology Committee. *Cancer Res* 2004;**64**:2270–305.
20 **Deshmumukh N**, Foster CS. Grading prostate cancer. In: Foster CS, Bostwick DG, eds. *Pathology of the prostate cancer*. Philadelphia: Saunders, 1998:191–227.
21 **Bostwick DG**. Neoplasms of the prostate. In: Bostwick DG, Eble JN, eds. *Urologic surgical pathology*. St Louis: Mosby, 1997:343–421.
22 **So WJ**, Cheville JC, Katzmann JA, *et al.* Factors that influence the measurement of prostate cancer DNA ploidy and proliferation in paraffin embedded tissue evaluated by flow cytometry. *Mod Pathol* 2001;**14**:906–12.
23 **Greenberg NM**, Demayo F, Finegold MJ, *et al.* Prostate cancer in a transgenic mouse. *Proc Natl Acad Sci U S A* 1995;**92**:3439–43.